



40 subglacial meltwater films (Kyrke-Smith et al., 2014). Numerous observations however, have
41 highlighted preferential location of ice streams at sites of specific bed properties such as in
42 topographic troughs, over areas of soft sedimentary geology, zones of higher geothermal heat
43 flux or as a consequence of where subglacial meltwater is routed (Winsborrow et al., 2010;
44 Kleiner et al., 2014). These viewpoints might not be mutually exclusive if self-organisation
45 into regularly-spaced streams is the primary control but that it is strongly mediated by local bed
46 templates (e.g. troughs) or events (meltwater drainage) that initiate or anchor streams in certain
47 locations. Exploring this hypothesis by numerical modelling has not yet been achieved because
48 of uncertainties in how to formulate basal ice flow in relation to bed friction, and due to
49 challenges of including all potentially relevant processes, especially so for subglacial water
50 flow (Flowers, 2015).

51 Observations of spatial and temporal variations in the activity of ice streams against
52 fluctuations in their subglacial hydrology suggest that the style and flux of water drainage is a
53 major component driving change. Examples include: reorganisation of subglacial drainage
54 systems (Elsworth and Suckale, 2016), subglacial water piracy, and development and migration
55 of transient subglacial water pockets (Gray et al., 2005; Peters et al., 2007; Siegfried et al.,
56 2016). However, these relations have been observed or inferred independently, at different
57 places and on yearly timescales, thus limiting our understanding of them of them as primary
58 drivers or as more minor effects of change. In this paper, we circumvent the challenge of
59 numerically modelling ice stream initiation and dynamics, including subglacial water drainage,
60 by exploiting a physical laboratory approach that simultaneously combines ice flow, water
61 drainage and bed erosion.

62 Connections between ice stream activity and subglacial hydrology are supported by the
63 occurrence of geomorphic markers of meltwater drainage on palaeo-ice stream beds (Margold
64 et al., 2015; Livingstone et al., 2016; Patterson, 1997). Among these landforms, tunnel valleys
65 deserve specific attention because they have high discharge capacities and, as such, may be
66 major contributors to the release of meltwater and sediment to the ocean; they may also promote
67 ice sheet stability by reducing the lubricating effect of high basal water pressure. Tunnel valleys
68 are elongated and over-deepened hollows, up to hundreds of kilometres long, several kilometres
69 wide and hundreds of meters deep. Their formation is generally attributed to subglacial
70 meltwater erosion but there is still no consensus on their development processes and on their
71 relationship to ice streaming. A conundrum being that ice streams appear to require high water
72 pressure while tunnel valleys are believed to involve low water pressure (Marczinek and
73 Piotrowski, 2006).

74 Ice streaming and tunnel valley development are both suspected to be linked to the
75 release of catastrophic glacial outburst floods at ice sheet margins (Bell et al., 2007; Hooke and
76 Jennings, 2006; Jørgensen and Piotrowski, 2003; Alley et al., 2006). Such outburst floods can
77 profoundly and rapidly alter the oceanic environment by transferring considerable amounts of
78 ice, freshwater and sediment from continents to oceans (Evatt et al., 2006). The suspected
79 connection between ice streams, tunnel valleys and outburst floods has never been observed or
80 modelled however.



81 Here, we describe the results of a physical experiment performed with an innovative analogue
82 modelling device that provides simultaneous constraints on ice flow, subglacial meltwater
83 drainage, subglacial sediment transport and subglacial landform development (Lelandais et al.,
84 2016; Fig. 1). From these results, we infer that ice streaming, subglacial meltwater pocket
85 migration, subglacial drainage reorganisation, tunnel valley formation and glacial outburst
86 floods are linked in influencing the location and dynamics of ice streams. This reconciles into
87 a single story several detached inferences, derived from observations at different timescales and
88 at different places on modern and ancient ice streams.

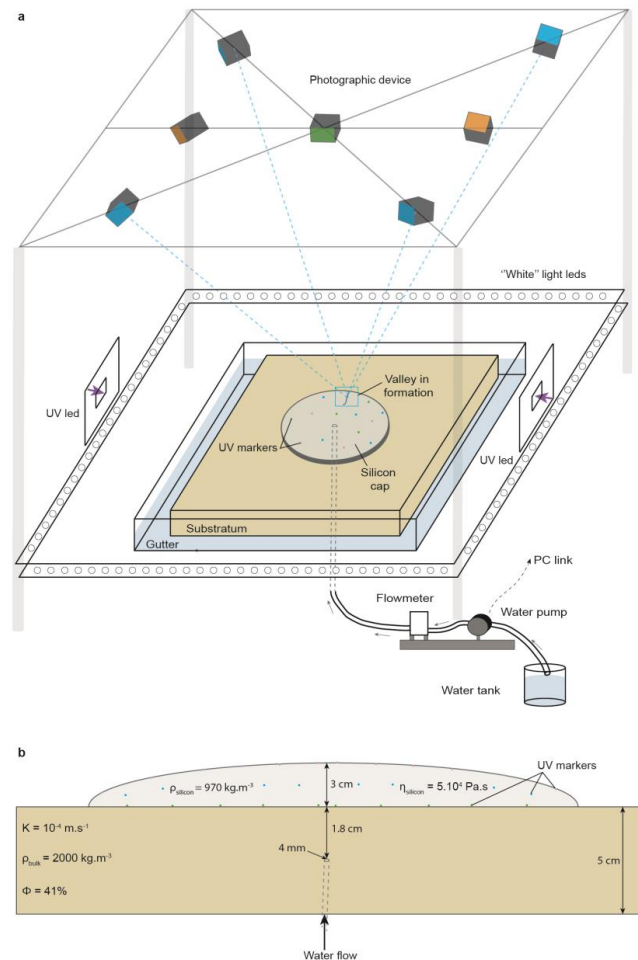
89 2. Experimental ice stream model

90 Ice stream dynamics are controlled by various processes that act at different space and time
91 scales; they also involve several components with complex thermo-mechanical behaviours (ice,
92 water, till, bedrock) (Hindmarsh, 2009). Considering all these processes and components
93 simultaneously is thus a challenge for modelling, especially with numerical computational
94 means (Fowler and Johnson, 1995; Marshall, 2005; Bingham et al., 2010). To overcome partly
95 this issue, we use an alternative experimental approach that allows simultaneous modelling of
96 ice flow, subglacial hydrology and sedimentary/geomorphic processes in a portion of an ice
97 sheet (Paola et al., 2009). Potentiometric surfaces that control subglacial water flow are
98 generally parallel to ice sheet surfaces (Fountain and Walder, 1998). Subglacial water drainage
99 is thus controlled by fluctuations in locations of ice sheet margins. The scaling of the experiment
100 is based on this rule and is designed to ensure that the value of the ratio between margin velocity
101 and incision rate of tunnel valleys in the experiment equals its value in natural systems (cf.
102 Lelandais et al., 2016 for scaling details).

103 The model is set in a glass box (70 cm long, 70 cm wide and 5 cm deep) (Fig. 1). A 5 cm thick,
104 flat, horizontal, permeable and erodible substratum, made of sand ($d_{50}=100\ \mu\text{m}$) saturated with
105 pure water and compacted to ensure homogeneous values for its density ($\rho_{\text{bulk}} = 2000\ \text{kg}\cdot\text{m}^{-3}$),
106 porosity ($\Phi = 41\ \%$) and permeability ($K = 10^{-4}\ \text{m}\cdot\text{s}^{-1}$), rests on the box floor. The ice sheet
107 portion is modelled with a 3 cm thick layer of viscous ($\eta = 5\cdot 10^4\ \text{Pa}\cdot\text{s}$) and transparent but
108 refractive ($n = 1.47$) silicon putty placed on the substratum. The model is not designed to
109 simulate an entire ice sheet; it is circular in plan view (radius = 15 cm) however, to avoid lateral
110 boundary effects on silicon flow. Subglacial meltwater production is simulated by injection of
111 water with a punctual injector, 4 mm in radius, placed at a depth of 1.8 cm in the substratum,
112 and connected to a pump (Fig. 1). The injector is located below the centre of the silicon layer
113 to be consistent with the circular geometry of the experiment. The water discharge is constant
114 ($1.5\ \text{dm}^3/\text{h}$) over the duration of the experiment and generates water flow at the silicon-
115 substratum interface and within the substratum. In contrast with ice, the commercial silicon
116 putty we use (Dow Corning, SGM36) is impermeable, Newtonian, isotropic, and its viscosity
117 is nearly independent of temperature between 10 and 30°C. Therefore, rheological softening of
118 ice with strain rate, temperature, anisotropy and meltwater content (Bingham et al., 2010)
119 cannot be reproduced. We did not try to include the equivalent of a till layer in the experiment,
120 although till deformation is known to promote ice streaming (Alley et al., 1987). The velocity
121 contrasts observed in the experiment are thus likely to be amplified, in natural ice sheets, by the
122 complex rheological behaviour of ice and till. This may lead to the development of narrower



123 ice streams with higher relative velocities and sharper lateral shear margins in natural ice sheets
 124 than in the experiment (Raymond, 1987; Perol et al., 2015).
 125



126

127 **Figure 1.** Description of the analog device used in this study. a, Overview of the analog device. The
 128 analog device consists in a 70 cm long, 70 cm wide and 5 cm deep glass box filled with saturated and
 129 compacted sand simulating the substratum. The ice sheet portion is simulated by a circular layer of
 130 silicon putty containing 3 levels of UV markers. Meltwater production is simulated by a central and
 131 punctual injection of pure water within the substratum. Five synchronized cameras placed above the
 132 silicon putty (in blue) focus on the tunnel valley system and are used to produce digital elevation models
 133 by photogrammetry. Another camera (in orange) takes overview photographs of the analog device to
 134 follow the progress of the whole experiment. A last camera (in green) is positioned at the vertical of the
 135 silicon layer centre and is configured to take high-resolution photographs in black light of the UV
 136 markers (illuminated with two lateral UV led lights). b, Cross-sectional profile of the analog device
 137 displaying the position of the UV markers and the physical characteristics of both the substratum and
 138 the silicon layer.



139 To monitor the vertical displacements of the silicon surface and the development of landforms
140 on its substratum, we use six synchronised cameras equidistant from the experiment centre: two
141 cameras (orange on Fig. 1) cover the whole extent of the experiment and four cameras (blue on
142 Fig. 1) focus on specific regions to obtain higher resolution images. These cameras take
143 simultaneous pictures with differing positions and orientations. Digital elevation models of the
144 silicon surface and of the substratum are derived from these images by photogrammetry.
145 Numerical post-treatments are performed on the digital elevation models to remove distortions
146 of the substratum topography due to light refraction in the silicon putty (cf detailed post-
147 treatment methods in Lelandais et al., 2016). Tests performed on previously known
148 topographies show that the vertical precision of the retrieved digital elevation models is better
149 than 10^{-1} mm.

150 The flow velocity of the silicon layer is monitored near its base (V_{base}), at mid-depth (V_{mid}) and
151 at its surface (V_{surface}), with an additional camera placed over the centre of the experiment (green
152 on Fig. 1). For that purpose, the camera records the horizontal position, on pictures taken at
153 regular time intervals in ultraviolet, of 180 paint drops (1 mm in radius) placed at 1 mm above
154 the base, at mid-depth and at the surface of the silicon layer (Fig. S1). These passive markers
155 are transparent at visible wavelengths and do not alter pictures of the substratum taken through
156 the silicon cap. They represent less than 0.5% of the silicon layer in volume and tests have
157 shown that they do not affect its overall rheological behaviour. Uncertainties in the measured
158 position of markers on images are less than one pixel in size (10^{-1} mm), thus uncertainties in
159 the derived velocities are comprised between $5 \cdot 10^{-4}$ and $2 \cdot 10^{-3}$ mm/s, depending on the time
160 interval between photographs.

161

162

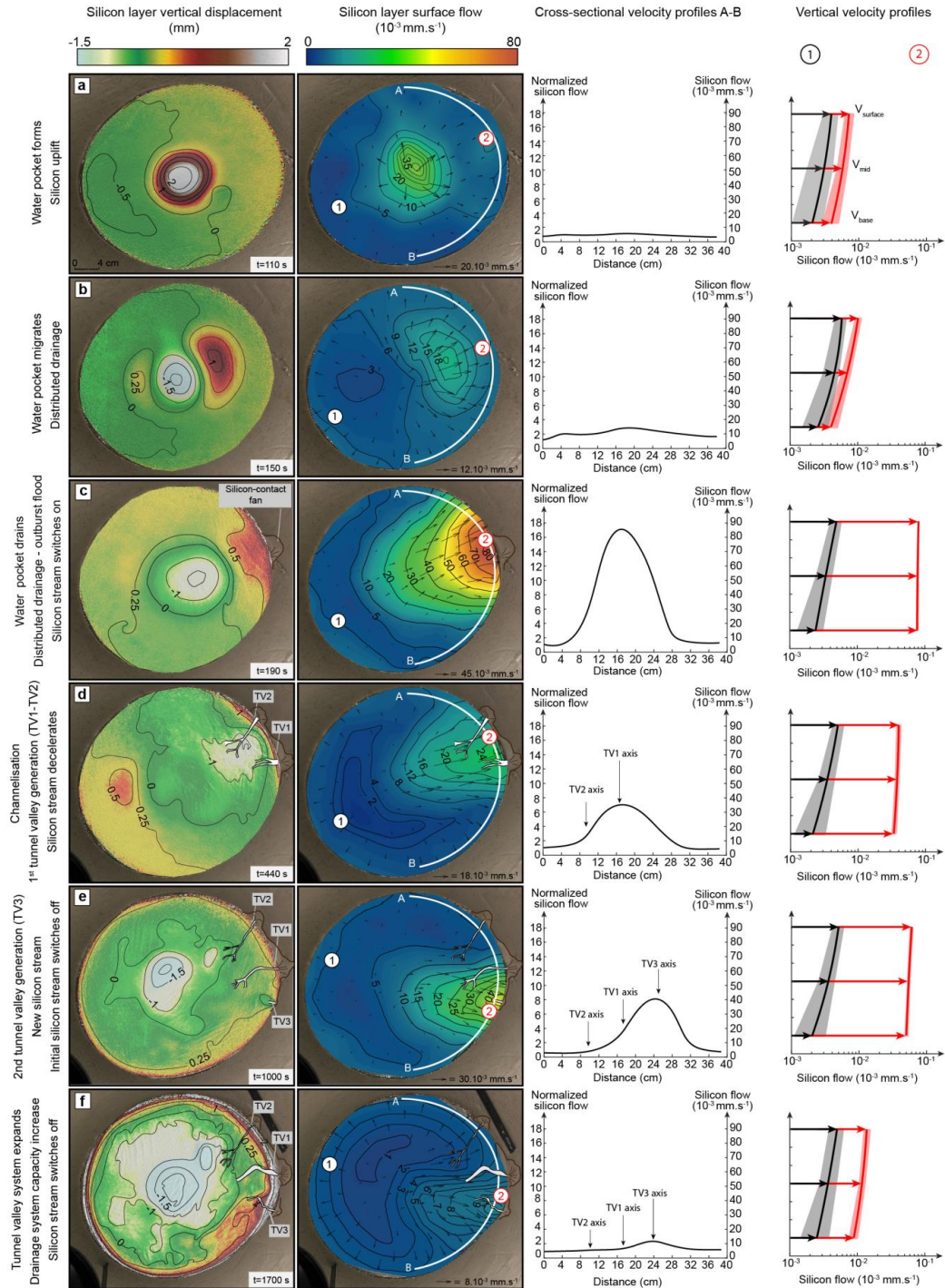
163

164

165

166

167





169 **Figure 2.** Temporal evolution of the experiment. a, Formation of water pocket, uplift of silicon surface
170 uplift and acceleration. b, Migration of water pocket and overlying region of uplift and accelerated flow.
171 c, Marginal drainage of water pocket and onset of silicon streaming. d, Tunnel valley development and
172 silicon stream deceleration. e, Formation, migration and marginal drainage of a new water pocket,
173 development of a second silicon stream and of a new tunnel valley. f, Decay of the second silicon stream.
174 From left to right: (i) maps of vertical displacements of silicon layer surface, (ii) maps of horizontal
175 velocity at silicon cap surface, (iii) cross-sectional velocity profiles (absolute velocity on right axis,
176 velocity normalised by background velocity on left axis, profile locations indicated by white lines A-B
177 on maps), (iv) vertical velocity profiles for silicon stream (red profiles, locations labelled 1 on maps)
178 and for region opposed to silicon stream (black profiles, locations labelled 2 on maps).

179 3. Experimental results

180 As long as no water is injected in the substratum, the silicon layer spreads under its own weight
181 and displays the typical parabolic surface profile of an ice sheet. It increases in diameter and
182 decreases in thickness with time, thus producing a radial pattern of horizontal velocities, which
183 increase in magnitude from the centre ($V_{\text{surface}} < 3 \cdot 10^{-3} \text{ mm} \cdot \text{s}^{-1}$) to the margin ($V_{\text{surface}} = 8 \cdot 10^{-3}$
184 $\text{mm} \cdot \text{s}^{-1}$) (Fig. S2). V_{base} is close to 0 over the full extent of the silicon layer ($\frac{V_{\text{base}}}{V_{\text{surface}}} \sim 0\%$),
185 indicating coupling with the substratum. The silicon flow pattern changes when meltwater
186 production is simulated by injecting water at a constant discharge ($1.5 \text{ dm}^3/\text{h}$), beneath the
187 silicon layer.

188 This experiment was repeated 12 times with identical input parameters. A six-stage ice stream
189 lifecycle linking outburst flooding, transitory ice streaming and tunnel valley development has
190 been observed for all these simulations (Fig. 2a-f, Fig. 4).

191 Stage 1 (Fig. 2a). A water pocket grows below the centre of the silicon layer and raises its
192 surface by 2 mm. Above the water pocket, the silicon accelerates ($V_{\text{surface}} \geq 35 \cdot 10^{-3} \text{ mm} \cdot \text{s}^{-1}$), and
193 is decoupled from the substratum ($\frac{V_{\text{base}}}{V_{\text{surface}}} = 75$ to 80%). Below the rest of the silicon layer,
194 lower velocities ($V_{\text{surface}} = 8 \cdot 10^{-3} \text{ mm} \cdot \text{s}^{-1}$, $\frac{V_{\text{base}}}{V_{\text{surface}}} = 40$ to 50%) indicate higher basal friction.
195 These results are consistent with inferences that meltwater ponding can form pressurised
196 subglacial water pockets associated with basal decoupling, surface uplift, and ice flow
197 acceleration in natural ice sheets (Elsworth and Suckale, 2016; Livingstone et al., 2016). In the
198 experiment however, these effects are restricted to an approximately circular region and are not
199 sufficient to produce channelised ice streaming.

200 Stage 2 (Fig. 2b). The water pocket expands and migrates towards the margin of the silicon
201 layer. The lack of channels incised in the substratum indicates that this displacement occurs as
202 distributed water drainage not accomplishing erosion. In the silicon layer, the region of surface
203 uplift, basal decoupling and acceleration ($V_{\text{surface}} = 18 \cdot 10^{-3} \text{ mm} \cdot \text{s}^{-1}$, $\frac{V_{\text{base}}}{V_{\text{surface}}} = 75$ to 85%)
204 expands and migrates downstream with the water pocket. Similar migrations of pressurised
205 subglacial water pockets have been observed or inferred under modern and ancient ice sheets
206 (Fricker et al., 2007; Carter et al., 2017), sometimes associated with migrations of regions of
207 ice surface uplift and ice flow acceleration (Bell et al., 2007; Stearns et al., 2008; Siegfried et



208 al., 2016). The experiment suggests that these water pockets can migrate by distributed drainage
209 and can contribute to the emergence of ice streams.

210 Stage 3 (Fig. 2c). When the water pocket reaches the margin of the silicon layer, it drains
211 suddenly. This marginal outburst flood is still fed by distributed drainage and conveys sand
212 particles eroded from the substratum towards a low-angle marginal sedimentary fan (Fig. S3).
213 Simultaneously, the silicon flow focuses in a stream (20 cm wide at the margin) that propagates
214 upstream from the silicon margin to the water injection area. This stream immediately peaks in
215 velocity ($V_{\text{surface}} = 80 \cdot 10^{-3} \text{ mm s}^{-1}$, 16 times higher than the surrounding silicon) and is entirely
216 decoupled from its substratum ($\frac{V_{\text{base}}}{V_{\text{surface}}} > 90\%$). Although similar relations between outburst
217 floods and ice flow accelerations have been suspected in modern (Alley et al., 2006; Bell et al.,
218 2007; Stearns et al., 2008) and past (Livingstone et al., 2016) ice sheets, they have been
219 documented for valley glaciers only (Kamb, 1985): there, they can produce sudden meltwater
220 discharges that exceed the capacity of distributed subglacial meltwater drainages and promote
221 basal decoupling and ice flow acceleration (Magnússon et al., 2007). The experiment confirms
222 that outburst floods can promote basal decoupling and trigger ice streaming in ice sheets
223 (Fowler and Johnson, 1995).

224 Stage 4 (Fig. 2d). The distributed subglacial drainage system starts to channelise: two valleys
225 (TV1 and TV2) appear below the margin of the silicon layer and gradually expand by regressive
226 erosion of the substratum. These valleys, with their constant widths, undulating long profiles
227 and radial distribution, are analogue to natural tunnel valleys in their dimensions, shapes and
228 spatial organization (Lelandais et al., 2016; Fig. S4). They are fed by distributed water drainage.
229 The sand eroded from the substratum transits through these valleys and accumulates in high-
230 angle marginal sedimentary fans, higher in elevation than the valley floors (Figs. 4 and S3-4).
231 In response to progressive channelisation of the water drainage into the expanding valleys, the
232 silicon stream narrows and slows down (12 cm wide at the margin; $V_{\text{surface}} = 24 \cdot 10^{-3} \text{ mm s}^{-1}$).
233 The silicon stream, still channelised, is still flowing 8 times faster than the rest of the silicon
234 layer and is still decoupled from the substratum ($\frac{V_{\text{base}}}{V_{\text{surface}}} > 85\%$). These results are consistent
235 with inferences that channelisation of hitherto distributed subglacial water drainage systems
236 can occur and reduce ice flow velocity after outburst floods (Magnússon et al., 2007; Kamb,
237 1987; Retzlaff and Bentley, 1993), and can be responsible for narrowing and deceleration of
238 ice streams (Raymond, 1987; Retzlaff and Bentley, 1993; Catania et al., 2006; Beem et al.,
239 2014; Kim et al., 2016). At this stage of the experiment, this transition, which corresponds to
240 the initiation of tunnel valleys, is not sufficient to stop ice streaming however.

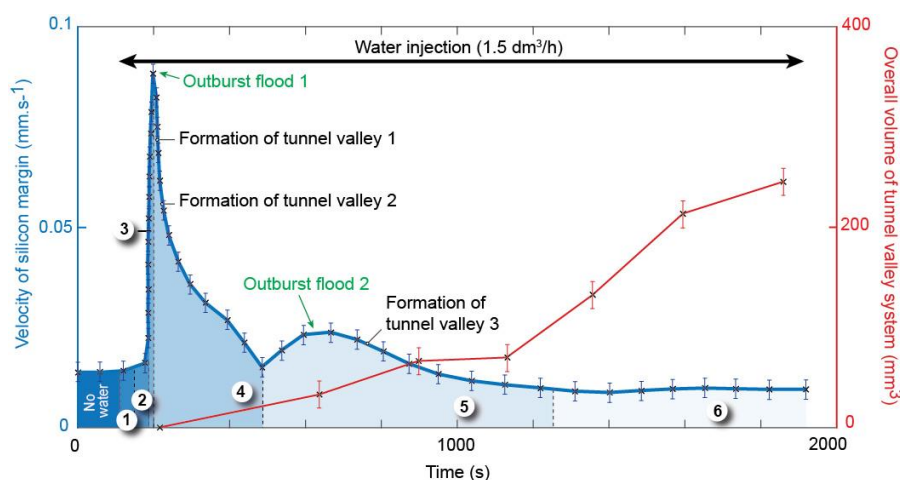
241 Stage 5 (Fig. 2e). A new transient water pocket grows below the silicon layer, migrates and
242 drains as an outburst flood, thus forming a new low-angle marginal sedimentary fan with at
243 lateral offset of 4 cm with respect to TV1. This induces the activation of a second stream (V_{surface}
244 $= 40 \cdot 10^{-3} \text{ mm s}^{-1}$) decoupled from its substratum ($\frac{V_{\text{base}}}{V_{\text{surface}}} = 80\%$) and the initiation of a new
245 radial valley (TV3), in a hitherto slow-moving region of the silicon cap. Simultaneously, the
246 first silicon stream switches off ($V_{\text{surface}} = 10 \cdot 10^{-3} \text{ mm s}^{-1}$), recouples to its substratum ($\frac{V_{\text{base}}}{V_{\text{surface}}} =$
247 30%), but water and sand still flow through TV1 and TV2. This result is consistent with



248 inferences that natural ice streams can switch on/off, surge or jump in location in response to
249 changes in subglacial water drainage reorganization (Beem et al., 2014; Hulbe et al., 2016;
250 Catania et al., 2012; Le Brocq et al., 2013). The experiment further suggests that this complex
251 behaviour is controlled by the growth and migration, in various possible directions, of transient
252 pressurised subglacial water pockets that form successively as long as the discharge capacity
253 of tunnel valleys systems is not sufficient to drain efficiently the available meltwater.

254 Stage 6 (Fig. 2f). Since their initiation, TV1, TV2 and TV3 have progressively increased in
255 width, depth and length. Their overall volume and discharge capacity have thus increased (Fig.
256 3). In response to this increased drainage efficiency, the second stream gradually decays (V_{surface}
257 $= 5 \cdot 10^3 \text{ mm.s}^{-1}$), recouples to its substratum ($\frac{V_{\text{base}}}{V_{\text{surface}}} = 35\%$), and the silicon layer ultimately
258 recovers a radial flow pattern (Fig. 2f). This result is consistent with the inference that ice
259 streams may decelerate and even switch off in response to reduction of subglacial water
260 pressures when efficient subglacial water drainage systems develop (Retzlaff and Bentley,
261 1993; Beem et al., 2014; Livingstone et al., 2016; Kim et al., 2016). In the experiment, this
262 development is governed by the expansion of tunnel valley networks.

263



264

265 **Figure 3.** Progressive expansion of overall volume of tunnel valleys system vs. velocity of silicon
266 margin through the experiment. The circled numbers correspond to the six-stages of the proposed ice
267 stream lifecycle.

268 4. Proposed lifecycle of transitory ice streams

269

270 The experiment demonstrates that, on flat and homogenous beds, ice streams may arise,
271 progress and decay in response to mechanical interactions between ice flow, subglacial water
272 drainage and bed erosion. On uneven or heterogeneous beds, these interactions may additionally
273 be enhanced or disturbed by spatial variations in the subglacial topography, geology and
274 geothermal heat flux (Bourgeois et al., 2000; Winsborrow, 2010). The complex rheology of
275 glacial ice and subglacial till (both generally soften with increasing strain rate, temperature,



276 water content and anisotropy) may also enhance these interactions by increasing velocity
277 contrasts between ice streams and their slower-moving margins (see methods for further
278 details). This may lead to the development of narrower ice streams with higher velocities and
279 sharper lateral shear margins in natural ice sheets than in the experiment (Raymond, 1987; Perol
280 et al., 2015).

281 Although the complexity of glacial systems cannot be fully modelled using the present
282 experimental setup, our results highlight the critical connection between ice streams and tunnel
283 valleys. This relation was suspected from the occurrence of tunnel valleys on palaeo ice stream
284 beds (Kehew et al., 2012; Ravier et al., 2015), but raised a contradiction: subglacial meltwater
285 pressures are classically believed to be high below ice streams (Bennett, 2003), while they are
286 suspected to be low in tunnel valleys (Marczinek and Piotrowski, 2006). Our results provide a
287 solution to this apparent contradiction: they demonstrate that ice streaming, tunnel valley
288 formation, release of marginal outburst floods and subglacial water drainage reorganization
289 may be interdependent parts of a single lifecycle that involves temporal changes in subglacial
290 meltwater pressures (Fig. 4).

291 1. Ice stream seeding. A prerequisite to the activation of ice streams is the formation of
292 pressurised subglacial pockets by meltwater ponding in ice sheet hinterlands. Approximately,
293 circular regions of surface uplift and accelerated ice flow develop above these transient water
294 pockets.

295 2. Ice stream gestation. Pressurised water pockets migrate downstream by distributed water
296 flow. Regions of surface uplift and accelerated ice flow migrate accordingly.

297 3. Ice stream birth. Once water pockets reach ice sheet margins, they drain as outburst floods.
298 At that time, ice streams switch on, peak in velocity and propagate towards ice sheet hinterlands
299 as decoupled corridors of accelerated ice flow underlain by pressurised distributed water
300 drainage.

301 4. Ice stream aging. Subglacial water drainage then channelises gradually: tunnel valleys fed by
302 pressurised distributed drainage start to form at ice stream fronts. Subsequent expansion of
303 tunnel valleys by regressive erosion progressively increases their overall discharge capacity,
304 lowers subglacial water pressures and provokes gradual ice stream recoupling and deceleration.

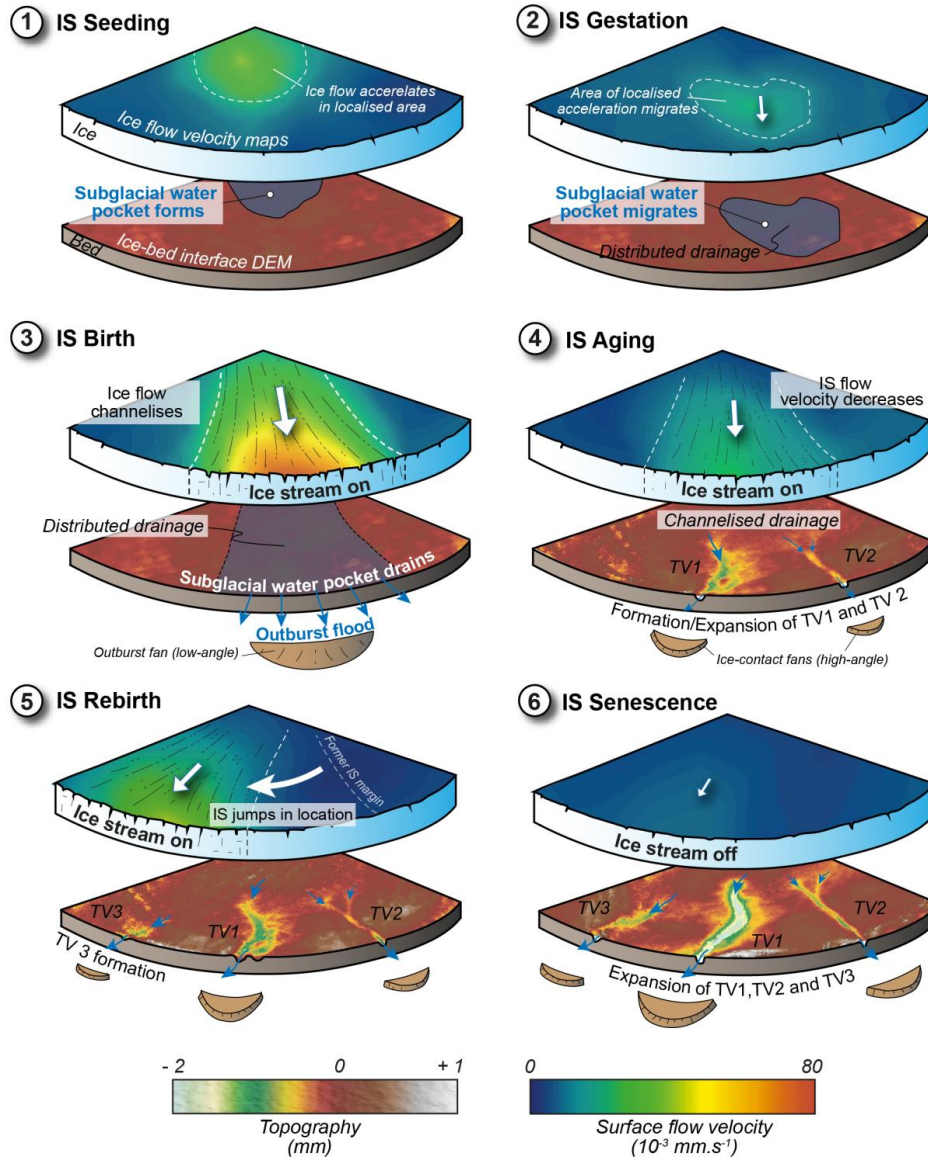
305 5. Ice stream rebirth (relocation or surge). As long as tunnel valley systems keep low drainage
306 capacities, successive pressurised subglacial water pockets can form, migrate and drain as
307 marginal outburst floods. On even and homogeneous ice sheet beds, subglacial water drainage
308 is controlled by the surface topography of ice sheets: subtle temporal changes in this topography
309 may thus be able to produce consecutive generations of ice streams and tunnel valleys at
310 different locations and with different flow directions. These jumps in locations and directions
311 may be responsible for the formation of independent, but sometimes intersecting, ice streams
312 corridors and tunnel valleys networks on some palaeo ice sheet beds (Jørgensen and Piotrowski,
313 2003; Fowler and Johnson, 1995). By contrast, if subglacial water routes and ice flow are
314 constrained by bed heterogeneities, migration of successive subglacial water pockets along
315 predetermined paths may induce sequential ice stream surges (Fowler and Johnson, 1995;



316 Hulbe et al., 2016) and participate in the gradual development of complex tunnel valley systems
317 at fixed places, like the Dry Valleys “Labyrinth” in Antarctica (Lewis et al., 2006).

318 6. Ice stream senescence. Ice streams may ultimately switch off when drainage capacities of
319 tunnel valley systems are sufficient to limit subglacial water overpressures. Tunnel valleys and
320 ice streams are frequently found to co-exist and with the many examples reported from
321 the southern margin of the Laurentide Ice Sheet (Patterson, 1997; Livingstone and Clark, 2016).
322 In one case, development of tunnel valleys has been suggested to have led to stagnation of ice
323 flow at an ice stream terminus (Patterson, 1997), a process that we have now demonstrated by
324 modelling. This further validates the hypothesis that tunnel valley development can secure ice
325 sheet stability by preventing catastrophic ice stream collapses (Marczinek and Piotrowski,
326 2006), which could represent early stages of unstoppable ice sheet disintegrations (Hulbe, 2017)
327 In a global change context, this possible stabilisation however requires that pre-existing and/or
328 newly forming tunnel valley systems expand sufficiently fast to accommodate increased
329 meltwater production. The processes and rates of tunnel valley development are thus major
330 issues for predicting the forthcoming behaviour of present-day ice sheets and for assessing their
331 contribution to the release of ice and freshwater to the ocean, which alters global sea level and
332 oceanic circulations.

333



334

335 **Figure 4.** Chronological sequence with interpretative sketches illustrating the proposed ice
 336 stream lifecycle and the relations with tunnel valley development. Basal topography and surface
 337 flow velocity maps are derived from the experiment.

338

5. Conclusion

339

340 The transitory and mobile nature of ice streams may be understood in the framework of
 341 a model lifecycle that involves temporal changes in subglacial meltwater pressures and arises
 from interactions between ice flow, subglacial water drainage and bed erosion. In this model



342 lifecycle transitory ice streams arise, progress and decay in response to subglacial flooding,
343 changes in type and efficiency of subglacial drainage, and development of tunnel valleys. These
344 results are consistent with (and reconcile) a variety of otherwise detached observations
345 performed at different timescales and at different places, on modern and ancient natural ice
346 streams. One of the most novel outcomes of this study, is that subglacial tunnel valley
347 development may be crucial in controlling ice stream vanishing and perhaps, as a consequence,
348 in preventing catastrophic ice sheet collapses during periods of climate change. The processes
349 and rates of tunnel valley development are thus major issues for predicting the forthcoming
350 behavior of present-day ice sheets and for assessing their contribution to the release of ice and
351 freshwater to the ocean. The innovative experimental approach, used here opens new
352 perspectives on the understanding of subglacial processes controlling ice sheet dynamics and
353 destabilisation

354 **Author contributions:**

355 OB, RM, ER and SP conceived this research and gathered funding. TL designed and conducted
356 the experiments (setup, monitoring and post-treatment), with contributions by RM and PS. TL,
357 ER, OB, CDC, SP and RM contributed to the interpretation of the results and of their natural
358 implications. TL wrote the first draft of the manuscript; ER, OB, SP and CDC contributed
359 substantially to its present version.

360 **Competing interests:**

361 The authors declare that they have no conflict of interest

362 **Acknowledgements:**

363 This study is part of the DEFORm project (Deformation and Erosion by Fluid Overpressure)
364 funded by “Région Pays de la Loire”. Additional financial support was provided by the French
365 “Agence Nationale de la Recherche” through grant ANR-12-BS06-0014 ‘SEQSTRAT-ICE’
366 and the “Institut National des Sciences de l’Univers” (INSU) through the ‘Programme National
367 de Planétologie’ (PNP) and ‘Système Terre : Processus et Couplages’ (SYSTER) programs.

368 **References**

- 369 Alley, R. B., Blankenship, D. D., Rooney, S. T., and Bentley, C. R.: Till beneath ice stream B:
370 4. A coupled ice-till flow model, *Journal of Geophysical Research*, 92, 8931-8940, 1987.
371
372 Alley, R. B., Dupont, T. K., Parizek, B. R., Anandkrishnan, S., Lawson, D. E., Larson, G. J.,
373 and Evenson, E. B.: Outburst flooding and the initiation of ice-stream surges in response to
374 climatic cooling: A hypothesis, *Geomorphology*, 75, 76-89, 2006.
375
376 Bamber, J. L., Vaughan, D. G., and Joughin, I.: Widespread complex flow in the interior of the
377 Antarctic Ice Sheet, *Science*, 287, 1248-1249, 2000.
378
379 Beckley, B.D., N.P. Zelensky, S.A. Holmes, F.G. Lemoine, R.D. Ray, G.T. Mitchum, S. Desai,
380 S.T. Brown, Assessment of the Jason-2 Extension to the TOPEX/Poseidon, Jason-1 Sea-



- 381 Surface Height Time Series for Global Mean Sea Level Monitoring, *Marine Geodesy*, 33(S1):
382 447-471, 2010.
383
- 384 Beem, L. H., Tulaczyk, S. M., King, M. A., Bougamont, M., Fricker, H. A., and Christoffersen,
385 P.: Variable deceleration of Whillans Ice Stream, West Antarctica, *Journal of Geophysical*
386 *Research: Earth Surface*, 119, 212-224, 2014.
387
- 388 Bell, R. E., Studinger, M., Shuman, C. A., Fahnestock, M. A., and Joughin, I.: Large subglacial
389 lakes in East Antarctica at the onset of fast-flowing ice streams, *Nature*, 445, 904-907, 2007.
390
- 391 Bennett, M. R.: Ice streams as the arteries of an ice sheet: their mechanics, stability and
392 significance, *Earth-Science Reviews*, 61, 309-339, 2003.
393
- 394 Bingham, R. G., King, E. C., Smith, A. M., and Pritchard, H. D.: Glacial geomorphology:
395 Towards a convergence of glaciology and geomorphology, *Progress in Physical Geography*,
396 34, 327-355, 2010.
397
- 398 Bourgeois, O., Dauteuil, O., and Van Vliet-Lanoë, B.: Geothermal control on flow patterns in
399 the last glacial maximum ice sheet of Iceland, *earth Surface Processes and Landforms*, 25, 59-
400 76, 2000.
401
- 402 Carter, S. P., Fricker, H. A., and Siegfried, M. R.: Antarctic subglacial lakes drain through
403 sediment-floored canals: theory and model testing on real and idealized domains, *The*
404 *Cryosphere*, 11, 381-405, 2017.
405
- 406 Catania, G. A., Scambos, T. A., Conway, H., and Raymond, C. F.: Sequential stagnation of
407 Kamb Ice Stream, West Antarctica, *Geophysical Research Letters*, 33, 1-4, 2006.
408
- 409 Catania, G., Hulbe, C., Conway, H., Scambos, T. A., and Raymond, C. F.: Variability in the
410 mass flux of the Ross ice streams, West Antarctica, over the last millennium, *Journal of*
411 *Glaciology*, 58, 741-752, 2012.
412
- 413 Elsworth, C. W. and Suckale, J.: Rapid ice flow rearrangement induced by subglacial drainage
414 in West Antarctica, *Geophysical Research Letters*, 43, 11,697-611,707, 2016.
415
- 416 Evatt, G. W., Fowler, A. C., Clark, C. D., and Hulton, N. R.: Subglacial floods beneath ice
417 sheets, *Philosophical transactions. Series A, Mathematical, physical, and engineering sciences*,
418 364, 1769-1794, 2006.
419
- 420 Flowers, G. E.: Modelling water flow under glaciers and ice sheets, *Proceedings. Mathematical,*
421 *physical, and engineering sciences*, 471, 20140907, 1-41, 2015.
422
- 423 Fountain, A. G. and Walder, J. S.: Water flow through temperate glaciers, *Reviews of*
424 *Geophysics*, 36, 299-328, 1998.
425
- 426 Fowler, A. C. and Johnson, C.: Hydraulic run-away: a mechanism for thermally regulated
427 surges of ice sheets, *Journal of Glaciology*, 41, 554-561, 1995.
428
- 429 Fricker, H. A., Scambos, T. A., Bindshadler, R., and Padman, L.: An active subglacial water
430 system in West Antarctica mapped from space, *Science*, 315, 1544-1548, 2007.



- 431
432 Gray, L.: Evidence for subglacial water transport in the West Antarctic Ice Sheet through three-
433 dimensional satellite radar interferometry, *Geophysical Research Letters*, 32, 1-4, 2005.
434
435 Hindmarsh, R. C. A.: Consistent generation of ice-streams via thermo-viscous instabilities
436 modulated by membrane stresses, *Geophysical Research Letters*, 36, 1-6, 2009.
437
438 Hooke, R. L. and Jennings, C. E.: On the formation of the tunnel valleys of the southern
439 Laurentide ice sheet, *Quaternary Science Reviews*, 25, 1364-1372, 2006.
440
441 Hulbe, C. L.: Is ice sheet collapse in West Antarctica unstoppable?, *Science*, 356, 910-911,
442 2017.
443
444 Hulbe, C. L., Scambos, T. A., Klinger, M., and Fahnestock, M. A.: Flow variability and ongoing
445 margin shifts on Bindschadler and MacAyeal Ice Streams, West Antarctica, *Journal of*
446 *Geophysical Research: Earth Surface*, 121, 283-293, 2016.
447
448 Jørgensen, F. and Piotrowski, J.: Signature of the Baltic Ice Stream on Funen Island, Denmark
449 during the Weichselian glaciation, *Boreas*, 32, 242-255, 2003.
450
451 Kamb, B.: Glacier surge mechanism based on linked cavity configuration of the basal water
452 conduit system, *Journal of Geophysical Research*, 92, 9083-9100, 1987.
453
454 Kamb, B., Raymond, C. F., Harrison, W. D., Engelhardt, H., Echelmeyer, K. A., Humphrey,
455 N., Brugman, M. M., and Pfeffer, T.: Glacier surge mechanism: 1982 - 1983 surge of
456 Variegated Glacier, Alaska, *Science*, 227, 469-479, 1985.
457
458 Kehew, A. E., Piotrowski, J. A., and Jørgensen, F.: Tunnel valleys: Concepts and controversies
459 - A review, *Earth-Science Reviews*, 113, 33-58, 2012.
460
461 Kim, B.-H., Lee, C.-K., Seo, K.-W., Lee, W. S., and Scambos, T.: Active subglacial lakes and
462 channelized water flow beneath the Kamb Ice Stream, *The Cryosphere*, 10, 2971-2980, 2016.
463
464 Kleiner, T. and Humbert, A.: Numerical simulations of major ice streams in Western Dronning
465 Maud Land, Antarctica, under wet and dry basal conditions, *Journal of Glaciology*, 60, 215-
466 232, 2017.
467
468 Kyrke-Smith, T. M., Katz, R. F., and Fowler, A. C.: Subglacial hydrology and the formation of
469 ice streams, *Proceedings. Mathematical, physical, and engineering sciences*, 470, 20130494, 1-
470 22, 2014.
471
472 Le Brocq, A. M., Ross, N., Griggs, J. A., Bingham, R. G., Corr, H. F. J., Ferraccioli, F., Jenkins,
473 A., Jordan, T. A., Payne, A. J., Rippin, D. M., and Siegert, M. J.: Evidence from ice shelves for
474 channelized meltwater flow beneath the Antarctic Ice Sheet, *Nature Geoscience*, 6, 945-948,
475 2013.
476
477 Lelandais, T., Mourgues, R., Ravier, É., Pochat, S., Strzeczynski, P., and Bourgeois, O.:
478 Experimental modeling of pressurized subglacial water flow: Implications for tunnel valley
479 formation, *Journal of Geophysical Research: Earth Surface*, 121, 2022-2041, 2016.
480



- 481 Lewis, A. R., Marchant, D. R., Kowalewski, D. E., Baldwin, S. L., and Webb, L. E.: The age
482 and origin of the Labyrinth, western Dry Valleys, Antarctica: Evidence for extensive middle
483 Miocene subglacial floods and freshwater discharge to the Southern Ocean. *Geology*, 34, 513-
484 516, 2006.
- 485
486 Livingstone, S. J. and Clark, C. D.: Morphological properties of tunnel valleys of the southern
487 sector of the Laurentide Ice Sheet and implications for their formation, *Earth Surface Dynamics*,
488 4, 567-589, 2016.
- 489
490 Livingstone, S. J., Utting, D. J., Ruffell, A., Clark, C. D., Pawley, S., Atkinson, N., and Fowler,
491 A. C.: Discovery of relict subglacial lakes and their geometry and mechanism of drainage,
492 *Nature communications*, 7, ncomms11767, 1-9, 2016.
- 493
494 Magnússon, E., Rott, H., Björnsson, H., and Pálsson, F.: The impact of jökulhlaups on basal
495 sliding observed by SAR interferometry on Vatnajökull, Iceland, *Journal of Glaciology*, 53,
496 232-240, 2007.
- 497
498 Marczynek, S. and Piotrowski, J. A.: Groundwater flow under the margin of the last
499 Scandinavian ice sheet around the Eckernförde Bay, northwest Germany, *Glacier science and
500 environmental change*, John Wiley & Sons, Knight, P. G., Blackwell Publishing, Oxford, UK,
501 60-62, 2006.
- 502
503 Margold, M., Stokes, C. R., Clark, C. D., and Kleman, J.: Ice streams in the Laurentide Ice
504 Sheet: a new mapping inventory, *Journal of Maps*, 11, 380-395, 2014.
- 505
506 Marshall, S.: Recent advances in understanding ice sheet dynamics, *Earth and Planetary
507 Science Letters*, 240, 191-204, 2005.
- 508
509 Paola, C., Straub, K., Mohrig, D., and Reinhardt, L.: The “unreasonable effectiveness” of
510 stratigraphic and geomorphic experiments, *Earth-Science Reviews*, 97, 1-43, 2009.
- 511
512 Patterson, C. J.: Southern Laurentide ice lobes were created by ice streams: Des Moines Lobe
513 in Minnesota, USA, *Sedimentary Geology*, 111, 249-261, 1997.
- 514
515 Payne, A. J. and Dongelmans, P. W.: Self-organization in the thermomechanical flow of ice
516 sheets, *Journal of Geophysical Research: Solid Earth*, 102, 12219-12233, 1997.
- 517
518 Perol, T. and Rice, J. R.: Shear heating and weakening of the margins of West Antarctic ice
519 streams, *Geophysical Research Letters*, 42, 3406-3413, 2015.
- 520
521 Peters, L. E., Anandakrishnan, S., Alley, R. B., and Smith, A. M.: Extensive storage of basal
522 meltwater in the onset region of a major West Antarctic ice stream, *Geology*, 35, 251, 2007.
- 523
524 Ravier, E., Buoncristiani, J.-F., Menzies, J., Guiraud, M., Clerc, S., and Portier, E.: Does
525 porewater or meltwater control tunnel valley genesis? Case studies from the Hirnantian of
526 Morocco, *Palaeogeography, Palaeoclimatology, Palaeoecology*, 418, 359-376, 2015.
- 527
528 Raymond, C. F.: How Do Glaciers Surge ? A Review, *Journal of Geophysical Research*, 92,
529 9121-9134, 1987.
- 530



- 531 Retzlaff, R. and Bentley, C. R.: Timing of stagnation of Ice Stream C, West Antarctica, from
532 short-pulse radar studies of buried surface crevasses, *Journal of Glaciology*, 39, 553-561, 1993.
533
- 534 Siegfried, M. R., Fricker, H. A., Carter, S. P., and Tulaczyk, S.: Episodic ice velocity
535 fluctuations triggered by a subglacial flood in West Antarctica, *Geophysical Research Letters*,
536 43, 2640-2648, 2016.
537
- 538 Stearns, L. A., Smith, B. E., and Hamilton, G. S.: Increased flow speed on a large East Antarctic
539 outlet glacier caused by subglacial floods, *Nature Geoscience*, 1, 827-831, 2008.
540
- 541 Vaughan, D.G., J.C. Comiso, I. Allison, J. Carrasco, G. Kaser, R. Kwok, P. Mote, T. Murray,
542 F. Paul, J. Ren, E. Rignot, O. Solomina, K. Steffen and T. Zhang, 2013: Observations:
543 Cryosphere. In: *Climate Change 2013: The Physical Science Basis. Contribution of Working*
544 *Group I to the Fifth Assessment Report of the Intergovernmental Panel on Climate Change*
545 *[Stocker, T.F., D. Qin, G.-K. Plattner, M. Tignor, S.K. Allen, J. Boschung, A. Nauels, Y. Xia,*
546 *V. Bex and P.M. Midgley (eds.)]. Cambridge University Press, Cambridge, United Kingdom*
547 *and New York, NY, USA*
548
- 549 Winsborrow, M. C. M., Clark, C. D., and Stokes, C. R.: What controls the location of ice
550 streams?, *Earth-Science Reviews*, 103, 45-59, 2010.
551
- 552
553
554
555
556
557
558